RESEARCH PAPER
https://doi.org/10.1071/FP21218

Functional Plant Biology

A *Panax notoginseng* phosphate transporter, PnPht1;3, greatly contributes to phosphate and arsenate uptake

Guan-hua Cao[A,#], Xi-fu Wang[A,#], Ze-dong Li[A], Xue Zhang[A], Xiao-gang Li[A], Wen Gu[A], Fan Zhang[A], Jie Yu[A,*] and Sen He[A,B,*]

For full list of author affiliations and declarations see end of paper

*Correspondence to:
Jie Yu
School of Chinese Materia Medica and Yunnan Key Laboratory of Southern Medicine Utilization, Yunnan University of Chinese Medicine, Kunming, Yunnan 650500, China
Email: cz.yujie@gmail.com and
Sen He
School of Chinese Materia Medica and Yunnan Key Laboratory of Southern Medicine Utilization, Yunnan University of Chinese Medicine, Kunming, Yunnan 650500, China
Email: senhe2019@outlook.com

#These authors contributed equally to this paper

Handling Editor:
Tim Cavagnaro

Received: 27 January 2021
Accepted: 17 December 2021
Published: 4 February 2022

Cite this:
Cao G *et al.* (2022)
Functional Plant Biology, **49**(3), 259–271.
doi:10.1071/FP21218

ABSTRACT

The crisis of arsenic (As) accumulation in rhizomes threatens the quality and safety of *Panax notoginseng* (Burk.) F.H. Chen, which is a well-known traditional Chinese herb with a long clinical history. The uptake of arsenate (AsV) could be suppressed by supplying phosphate (Pi), in which Pi transporters play important roles in the uptake of Pi and AsV. Herein, the *P. notoginseng* Pi transporter-encoding gene *PnPht1;3* was identified and characterised under Pi deficiency and AsV exposure. In this study, the open reading frame (ORF) of *PnPht1;3* was cloned according to RNA-seq and encoded 545 amino acids. The relative expression levels revealed that *PnPht1;3* was significantly upregulated under phosphate deficiency and AsV exposure. Heterologous expression in *Saccharomyces cerevisiae* MB192 demonstrated that *PnPht1;3* performed optimally in complementing the yeast Pi-transport defect and accumulated more As in the cells. Combined with the subcellular localisation prediction, it was concluded that *PnPht1;3* encodes a functional plasma membrane-localised transporter protein that mediates putative high-affinity Pi/H^+ symport activity and enhances the uptake of Pi and AsV. Therefore, a better understanding of the roles of the *P. notoginseng* Pi transporter could provide new insight for solving As accumulation in medicinal plants.

Keywords: arsenate (AsV) exposure, arsenic (As) acquisition and accumulation, heterologous expression, molecular mechanism, *Panax notoginseng*, phosphate (Pi) transporter, Pi deficiency, relative expression level.

Introduction

Panax notoginseng (Burk.) F.H. Chen is a commonly used traditional Chinese herb, of which the rhizome is a historically and officially utilised medicinal part that has been used for hundreds of years in clinical treatment (Kim 2018; Xiong *et al.* 2019). The primary bioactive constituents are saponins, mainly consisting of ginsenosides Rb1 and Rg1 and notoginsenoside R1. All are classified as dammarane-type tetracyclic triterpenoids (Zu *et al.* 2018). Evidence showed that notoginsenoside has therapeutic effects on dissipating blood stasis and arresting bleeding, thereby promoting the subsidence of swelling and relieving pain (Ou *et al.* 2016). Unfortunately, arsenic (As) contamination increases the drug-use risk of *P. notoginseng*, mainly caused by high As background concentrations in the soil and wide-scale use of As-containing pesticides (Zhu *et al.* 2017). Investigations found that total As concentrations in organs of *P. notoginseng* and their preparation planted in Wenshan Autonomous Prefecture occasionally exceeded the threshold value of 2.0 mg/kg listed in the As standard of China Green Trade Standards of Importing and Exporting Medicinal Plants and Preparation, and the concentrations in excess of the maximum permissible level were as high as 24%, 81% 14%, 57%, 44% and 56% in rhizomes, fibrous roots, stems, leaves, seeds and preparation, respectively, causing a serious health risk (Yan *et al.* 2011; Lin *et al.* 2013). As a highly toxic heavy metal, arsenic is listed at the top of the world's top 10 most toxic hazardous substances by the 'Agency for Toxic Substances and Disease Registry' (ATSDR) (Li *et al.* 2008;

Jedynak *et al.* 2010), which could pose a serious threat to human health through the food chain. Thus, it would be a major health threat if *P. notoginseng* was utilised in clinical treatment.

Due to similar chemical characteristics and competition relationships between phosphate (Pi) and arsenate (AsV), supplementation with Pi suppresses the As uptake in plants (Woolson *et al.* 1973; Cao *et al.* 2003; Sun *et al.* 2020). This theory has been proved in *Pteris vittata* L. (Huang *et al.* 2007; Lei *et al.* 2012) and *Pennisetum clandestinum* Hochst (Panuccio *et al.* 2012), where phosphorus (P) addition reduced As translocation and accumulation. As a macronutrient, P is involved in some key biological functions in plant growth; e.g. structural cell components, energy transfer and photosynthesis (Knudson *et al.* 2003; Rufyikiri *et al.* 2006). Soil P in various forms and organic and inorganic weathering are taken up by Pi transporters (Pht) in the plants, which are usually driven by the generation of a proton gradient (Shen *et al.* 2011; Qin *et al.* 2012*a*; Doki *et al.* 2013; Li *et al.* 2019; Wang *et al.* 2019).

Pi transporters are usually categorised into high- and low-affinity types based on Km values. High-affinity Pi transporters with a Km value of micromoles are usually induced by Pi deficiency (López-Arredondo *et al.* 2014; Wang *et al.* 2019), while low-affinity Pi transporters are constitutive proteins with a millimolar Km value (López-Arredondo *et al.* 2014). Evidence suggested that plant Pi transporters consist of Pht1, Pht2, Pht3, Pht4 and PHO1 (PHOSPHATE 1), the first four of which were reported to localise in the plasma membrane, plastid inner membrane, mitochondrial inner membrane and Golgi compartment, respectively (Mimura 1999; Rausch *et al.* 2001; Liu *et al.* 2011). Numerous studies found that Pht-type proteins (Pht1, Pht2, Pht3 and Pht4) are mainly expressed in the epidermis and cortical tissue of the root hair zone under the stress of Pi deficiency and contribute to Pi uptake (Shin *et al.* 2004; Qin *et al.* 2012*b*). To date, many plant Pi transporters have been implicated in the uptake of Pi and AsV; e.g. PvPht1;3 from *P. vittata* (Ditusa *et al.* 2016), PHT1;3, PHT1;4 and PHT1;12 from *Salix* spp. (Puckett *et al.* 2012). Moreover, it is a common way of tolerance employed for As resistance by suppressing Pi/AsV uptake on the basis of the interplay between AsV uptake and Pi nutrition (Puckett *et al.* 2012).

Currently, the roles of *P. notoginseng* Pi transporters in the uptake of Pi and AsV are still unclear under the stress of Pi deficiency and As exposure. In this work, we identified a *P. notoginseng* Pi transporter-encoding gene, *PnPht1;3*, and uncovered the expression characteristics at the transcriptional level. In addition, an ideal approach to uncover the mechanism of Pi/AsV uptake is to employ mutant *Saccharomyces cerevisiae* MB192, which significantly reveals this uptake with Pi–AsV interplay. Our work helps to illustrate the role of *P. notoginseng* Pi transporters in the uptake of Pi and AsV; therefore, it will be useful for decreasing As accumulation in the rhizome.

Material and methods

Experimental materials and setups

One-year-old *Panax notoginseng* (Burk.) F.H. Chen seedlings with non-significant in biomass (fresh weight, leaf number and plant height) were selected as treatment materials, and grew well at a standard garden Wenshan Prefecture Yunnan Province. These *P. notoginseng* were authenticated by professor Rong-hua Zhao (Yunnan University of Chinese Medicine). Growing media in garden pots consisted of 10% silt, 20% light aggregate, 30% clay and 40% expanded vermiculite (Mandal *et al.* 2015), in which dissolved phosphorus content was cut down to an extremely low level by washing with 1% $NaHCO_3$. Then, dissolved phosphorus concentrations were adjusted to 0.07 mM (low P, lP), 0.7 mM (medium P, mP) and 1.4 mM (high P, hP) by adding KH_2PO_4 (Cao *et al.* 2020). Before planting, sodium arsenate (Na_3AsO_4) was thoroughly mixed into media with a 0.2 mM final concentration in dry weight for As treatment groups. The As concentration is in line with the background value of soil in Wenshan Prefecture Yunnan Province, where is the main producing area (Feng *et al.* 2005). In this experiment, there were six treatments in total, including lPnAs (low P, no As), lPhAs (low P, high As), hPnAs (high P, no As), hPhAs (high P, high As), mPhAs (med P, high As) and mPnAs (med P, no As; CK). Due to the absence of mineral nutrition caused by repeatedly media-washed, 50 mL 1/4 Hoagland solution without P was added to nourish *P. notoginseng* regularly. The growing environment of *P. notoginseng* was extremely strict in the greenhouse, keeping 25°C and 85% relative humidity, and protecting against direct sunlight and water-accumulated. After 5 months, the fresh fibrous roots of *P. notoginseng* were collected for RNA extraction. Eight biological replicates were included in each treatment, and four samples were in every replicate.

Clone of *PnPht1;3*

Open reading frame (ORF) sequence of *PnPht1;3* was first obtained from a transcript of *P. notoginseng* fibrous roots treated as above described. The primer pair of *PnPht1;3* for ORF amplification were listed in Table 1. The first-strand cDNA was used as a template, which was gained by reverse transcription from total RNA with Primescript II 1st strand cDNA synthesis kit (Takara, Japan). Total RNA was extracted from the fibrous roots according to the protocol of miniBEST plant RNA extraction kit (TaKaRa, Japan). The PCR programme for the *PnPht1;3* consisted of initial denaturation step (94°C/5 min), followed by 35 cycles of 94°C/1 min, 58°C/30 s, 72°C/1 min, holding at 4°C.

Table 1. Primer pairs used for ORF cloning, qPCR, and recombinant plasmid construction.

Genes	Primers (5′–3′)	Usage
PnPht1;3	F: ATGGCTAGAGAACAA CTGGAAG	To amplify cDNA ORF
	R: TTAAACTGGAACGGT CCTAGTG	
qPnPht1;3	F: GCGTTTTGTGGCACTCTTGC	To amplify segments for qPCR
	R: TTTTTGTTGGCGTATTCGGA	
26S-2 (reference gene)	F: CAGTATTTAGCCTTGGA CGGAATT	
	R: CGGGTTGTTTGGGAATGC	
SPnPht1;3 (*Bam*HI/*Kpn* I)	F: CGCGGATCCATGGCTAGA GAACAACTGGAAG	To amplify genes for recombinant plasmid construction in *S. cerevisiae*
	R: CGGGGTACCTTAAACTGGA ACGGTCCTAGTG	

Quantitative real-time PCR

The relative expression levels of *PnPht1;3* in different treatment groups were validated by quantitative real-time polymerase chain reaction (qPCR) with TB Green *Premix Ex Taq* (Tli RNaseH Plus), ROX plus (TaKaRa, Japan). Primer pairs of *PnPht1;3* and reference gene (*26S-2*) (Wu *et al.* 2015) were also listed in the Table 1. The qPCR result of *PnPht1;3* was calculated using the formula $2^{-\Delta\Delta Ct}$ (Livak and Schmittgen 2001).

Identification and phylogenetic analyses

The ORF of *PnPht1;3* was authenticated via online software at https://www.ncbi.nlm.nih.gov/orffinder/. Biological information, including the location of hydrophobic, isoelectric point, protein molecular weight and putative transmembrane domains were predicted with the software package mounted at http://expasy.org/tools/protscale.html. The prediction of subcellular localisaiton was performed at http://wolfpsort.hgc.jp/. Multiple peptide alignments were analysed with DNAMAN v6.0. Phylogenetic tree was constructed using MEGA ver. 7.0 software with a parameter of 1000 bootstrap replications. The sequence of *PnPht1;3* has been submitted to NCBI and assigned a GenBank accession number MT406774.

Functional complementation assay of *PnPht1;3* in yeast

Mutant yeast, *Saccharomyces cerevisiae* MB192 (*MATa* pho3-1 pho84::HIS3 ade2 leu2-3, 112 his3-532, trp1-289 ura3-1, 2 can1) was used as a heterologous expression tool for uptake-functional verification, of which the high-affinity Pi transporter gene *PHO84* is knocked-out, and inserted an HIS3 DNA fragment *in situ* (Bun-Ya *et al.* 1991; Qin *et al.* 2012*a*). The full-length of *PnPht1;3* was amplified with primers containing restriction enzyme cutting sites are listed in Table 1. The amplicon was digested with *Bam*HI/*Kpn* I, and then attached to the expression vector YEplac112 digested with corresponding enzymes using T4 DNA Ligase (NEB, USA). The recombinant plasmid and empty vector YEplac112 were transformed into *S. cerevisiae* MB192 by electro-transformation (Costaglioli *et al.* 1994). Two types recombinant yeasts were obtained, and named MB192-*PnPht1;3* and MB192-YEplac112.

For the effect of Pi concentrations on the growth of yeasts, monoclonal cells were first cultured to the logarithmic phase (OD_{600} = 0.6) in the YNB liquid medium. Then, 100 μL suspension liquid were diluted to 5 mL by adding YNB medium, and cultured at 200 rpm and 30°C. The medium were adjusted to different Pi concentrations, including 0.002, 0.02, 0.06, and 0.1 mM with the same initial pH of 6.8 (Liu *et al.* 2014*b*). Bromocresol purple was used as a pH indicator in the medium, which shift a colour change from light yellow to purplish-red within a pH range of 5.2–6.8. The change of pH was affected by the concentration of cells and acid phosphatase (ACP) activity (Jia *et al.* 2011). For pH-dependent Pi uptake experiments, identified cells were cultured in the YNB liquid medium containing 80 μM Pi for 24 h at 200 rpm and 30°C, and the initial pH values were adjusted to 4, 5, 6, 7 and 8, respectively. For the determination of growth curve and growth rate, OD_{600} of yeast cells was determined every 3 or 5 h culturing in 5 mL SD-Trp$^-$ medium at 200 rpm and 30°C, of that the medium contained 20 μM Pi and 2% glucose with a pH value of 6 and an initial OD_{600} of 0.03 (Ditusa *et al.* 2016). Growth rate coefficients of logarithmic phase of yeast cells were calculated via exponential regression.

Pi uptake of transformants affected by respiratory inhibitors

The 100 μL yeast suspension (OD_{600} = 0.6) was diluted into 5 mL SD-Trp$^-$ medium containing 2% glucose and 80 μM KH_2PO_4, and adjusted an initial pH to 6.0, with or without carbonyl cyanide *m*-chlorophenylhydrazone (CCCP) (10, 50 μM) or 2,4-dinitrophenol (2,4-DNP) (100, 200 μM) (Mitsukawa *et al.* 1997; Zhang *et al.* 2014). CCCP should be initially dissolved in ethanol, and then added into the medium with a final concentration of 0.01% (v/v) (Li *et al.* 2008). Growth density was measured after shake cultivation for 20 h at 200 rpm, 30°C.

Effect of Pi concentrations on AsV uptake

For the growth rate and As tolerance of yeast cells, exponential yeast suspension of MB192-*PnPht1;3* and MB192-YEplac112 were inoculated into 10 mL SD-Trp$^-$

medium containing 50 μM Pi and 2% glucose, respectively, that made an initial OD_{600} to 0.03. Then, AsV was mixed into the medium with a final concentration of 80 μM before culturing at 200 rpm and 30°C. The OD_{600} of transformants was determined every 3 or 5 h for analysing growth rate coefficients and AsV tolerance during logarithmic phase (Ditusa *et al.* 2016). To investigate the effect of Pi concentrations on the As uptake of transformants, the OD_{600} and total As concentrations of MB192-*PnPht1;3*, MB192-YEplac112, mutant MB192 and wild type (WT) yeast cells were determined. Firstly, 1 mL yeast suspension (OD_{600} = 0.6) were transferred into 50 mL SD-Trp$^-$ medium containing 2% glucose, 20/100 μM Pi and 80 μM AsV, and then adjusted their initial pH to 6.0. Determination of OD_{600} of yeast suspension was carried out after shake cultivation at 200 rpm and 30°C for 30 h. Then, yeast cells were collected by centrifuging at 5000 rpm for 5 min, and the cell pellets were washed twice with 25 mL 10 mM EDTA for removing adhered As (Gravot *et al.* 2004). The total As concentrations in cells were determined via inductively coupled plasma mass spectrometry (ICP-MS) (Agilent 7500c, USA) as described by Wu *et al.* (2011) and Xu *et al.* (2017), in which yeast samples were ground to fine powder with liquid nitrogen and digested with HNO_3:H_2O_2 (85:15, v/v). Data used for analysing were performed with four biological replicates, and three technical replications in each biological replicate were conducted independently.

Statistical analysis

All data collected were processed and analysed statistically with SPSS 17.0 and Sigmaplot 12.0. The method of significant difference was the Turkey HSD tests of one-way analysis of variance (ANOVA) at the level of 0.05, that was conducted based on the assumptions of normality and homogeneity of variances, including qPCR result, ACP activity, OD_{600}, As concentration, growth rate coefficient and AsV tolerance. An independent-samples *t*-test at the 0.05 or 0.01 level was also employed to analyse the difference, including OD_{600} between each treatment (CCCP or 2,4-DNP) and CK, OD_{600} or As concentrations between 20 μM and 100 μM Pi. Data used in figures were expressed as the means ± standard deviation (s.d., $n \geq 3$).

Results

PnPht1;3 encodes Pi transporter 1

The ORF length of *PnPht1;3* cDNA is 1605 bp; and the predicted translation product consists of 535 amino acids with a calculated molecular mass and isoelectric point of 59.04 kDa and 8.87, respectively. Transporter PnPht1;3 contains 10 transmembrane domains and a Pht1 signature sequence (GGDYPLSATIxSE) (Karandashov and Bucher 2005) in a red-line box, as shown in Fig. 1. Peptide sequence alignment of the PnPht1;3 and other Pi transporters revealed that PnPht1;3 shared 84.83%, 84.83%, and 70.24% identity with NtPht1 (GenBank accession number, AF156696.1), CmPht1 (QAU07451.1), and PvPht1;3 (KM192137.1), respectively (Fig. 1).

To investigate the evolutionary relationship of PnPht1;3 with other homologues, a phylogenetic analysis was performed using the MEGA ver. 4.0 programme (Fig. 2). The results demonstrate that PnPht1;3, PvPht1;3 and CmPht1 belong to the Pht1 subfamily. In addition, subcellular localisation prediction showed that *PnPht1;3* located in the plasma membrane. These results demonstrate that *PnPht1;3* may be closely related to the uptake of Pi in *P. notoginseng*.

Relative expression levels of *PnPht1;3* in the roots of *P. notoginseng* under Pi deficiency and As exposure stress

In Fig. 3, it was found that *PnPht1;3* significantly responded to Pi deficiency, and the fold change in expression became larger with AsV supplementation in the low-concentration Pi treatment groups; e.g. 24.8-fold increase with lPnAs and 81.7-fold increase with lPhAs. In addition, compared with low-concentration Pi (lP) treatment, the expression level of *PnPht1;3* sharply decreased by supplementation with sufficient phosphate and presented a significant difference; e.g. a 24.8-fold increase with lPnAs, a 1-fold increase with mPnAs (CK), and a 0.9-fold decrease with hPnAs. The fold changes of mPhAs and hPhAs were 0.5 and 2.2, respectively, and were significantly less than 81.7 for lPhA, indicating that a high-concentration of Pi also weakened the stress of AsV. These results suggest that transporter PnPht1;3 may be involved in the uptake of Pi and AsV, and the supplementation with a high-concentration of Pi may decrease the stress caused by Pi deficiency or AsV exposure.

Complementation tests in *S. cerevisiae* MB192

Heterologous expression of *PnPht1;3* in mutant yeast MB192 supported its survival at low concentrations of Pi (0.002 mM and 0.02 mM) by improving Pi uptake. The OD_{600} of strain MB192-*PnPht1;3* was remarkably higher than that of MB192 and MB192-YEplac112, particularly at low concentrations of Pi, close to that of the WT type. The logarithmic phase of MB192-*PnPht1;3* was 10–25 h (Fig. 4*a*). The colour of medium-cultured MB192-*PnPht1;3* and WT cells was yellow at 0.002 mM, 0.02 mM, and 0.06 mM Pi, while MB192 and MB192-YEplac112 cells were purple or faint yellow under low-Pi conditions (0.002 mM, 0.02 mM, and 0.06 mM) (Fig. 4*b*). This change in medium colour is in accordance with the pH value and ACP activity of yeast cells. As shown in Fig. 4*c*, the ACP activity of MB192-*PnPht1;3* was higher than that of MB192-YEplac112 and

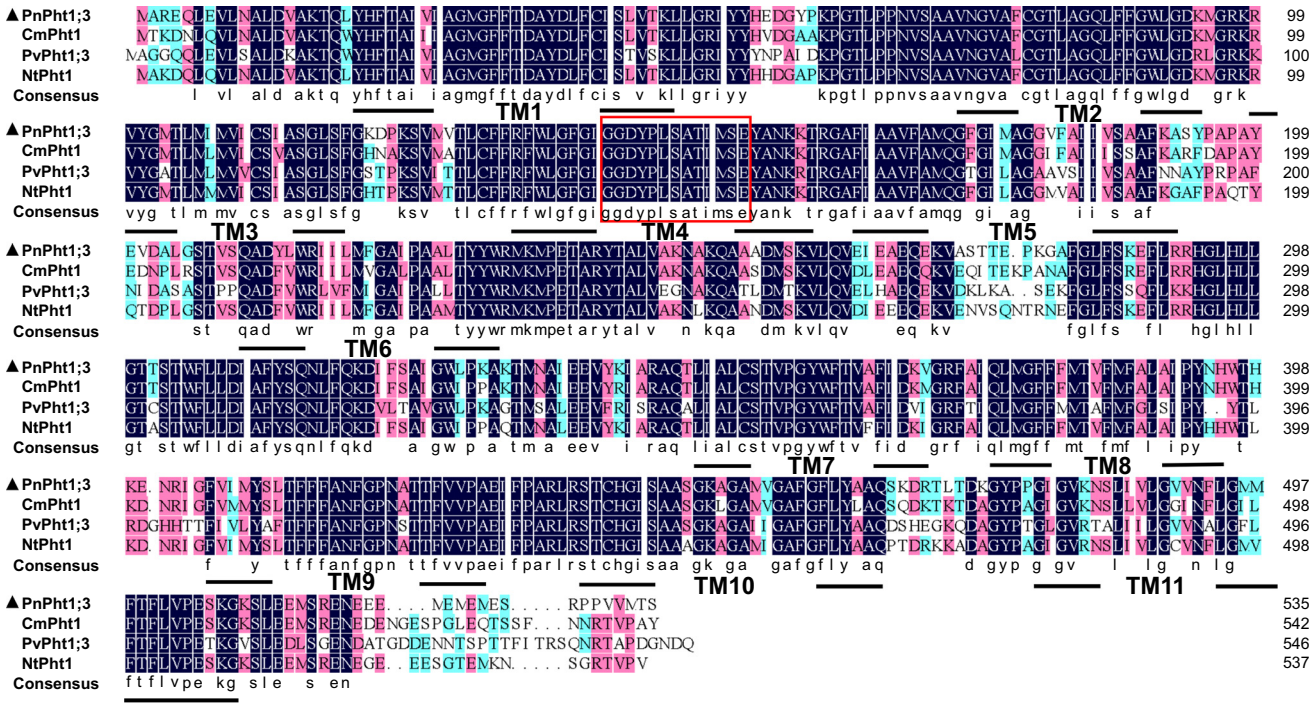

Fig. 1. Alignment of PnPht1;3 and the peptide sequences of known Pi transporters present in *Nicotiana tabacum* L. (NtPht1, AF156696.1), *Castanea mollissima* BL. (CmPht1, QAU07451.1) and *P. vittata* (PvPht1;3, KM192137.1). Identical peptides are highlighted in black, and conservative substitutions are highlighted in pink. Predicted transmembrane domains of PnPht1;3 were marked by underlines. The signature sequence of Pht1 is shown in a red box.

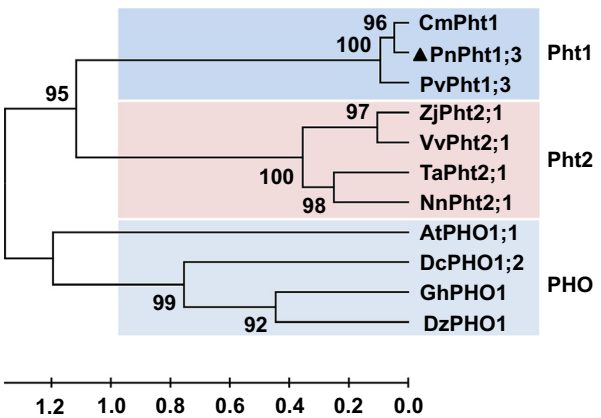

Fig. 2. Phylogenetic relationship of PnPht1;3 and other plant Pi transporters. CmPht1 (QAU07451.1) from *C. mollissima*; PvPht1;3 (KM192137.1) from *P. vittata*; ZjPht2;1 (XP_015894666.1) from *Ziziphus jujuba* Mill.; VvPht2;1 (XP_002271876.1) from *Vitis vinifera* L.; TaPht2;1 (AY293827.1) from *Triticum aestivum* L.; NnPht2;1 (XM_010250335.2) from *Nelumbo nucifera* Gaertn.; AtPHO1;1 (NM_113246.5) from *Arabidopsis thaliana* L.; DcPHO1;2 (XM_017360779.1) from *Daucus carota* var. sativus Hoffm.; GhPHO1 (XM_016884382.1) from *Gossypium hirsutum* L.; DzPHO1 (XM_022904580.1) from *Durio zibethinus* Merr. The bootstrap value was calculated with 1000 replications.

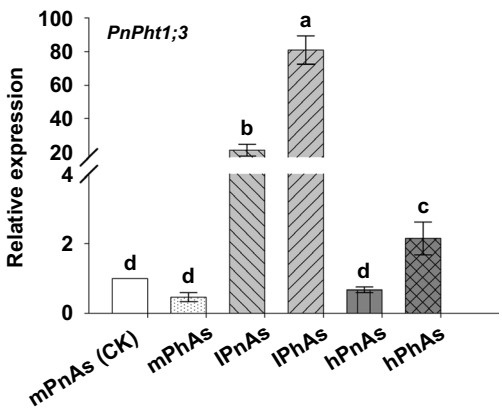

Fig. 3. Relative expression levels of *PnPht1;3* in fibrous roots of *P. notoginseng* under the stress of Pi deficiency and AsV exposure. One-year-old *P. notoginseng* plants in good condition were treated with different phosphate concentrations [(KH_2PO_4), 0.07 mM (lP), 0.7 mM (mP), and 1.4 mM (hP)] and supplemented with or without 0.20 mM AsV (Na_3AsO_4). The treatment of mPnAs (0.7 mM Pi and non-AsV) was set as a control group. Different lowercase letters represent difference of *PnPht1;3* among different treatments, $P \leq 0.05$. Error bars indicate mean values ± s.d. ($n = 4$).

MB192 and presented a significant difference ($P < 0.05$). The optimal pH value for MB192-*PnPht1;3* and WT was 6 (Fig. 4*d*). In addition, the OD_{600} of MB192-*PnPht1;3* cells was significantly suppressed by supplementation with the respiratory inhibitors CCCP and 2,4-DNP. This phenomenon became more obvious with increasing respiratory inhibitor

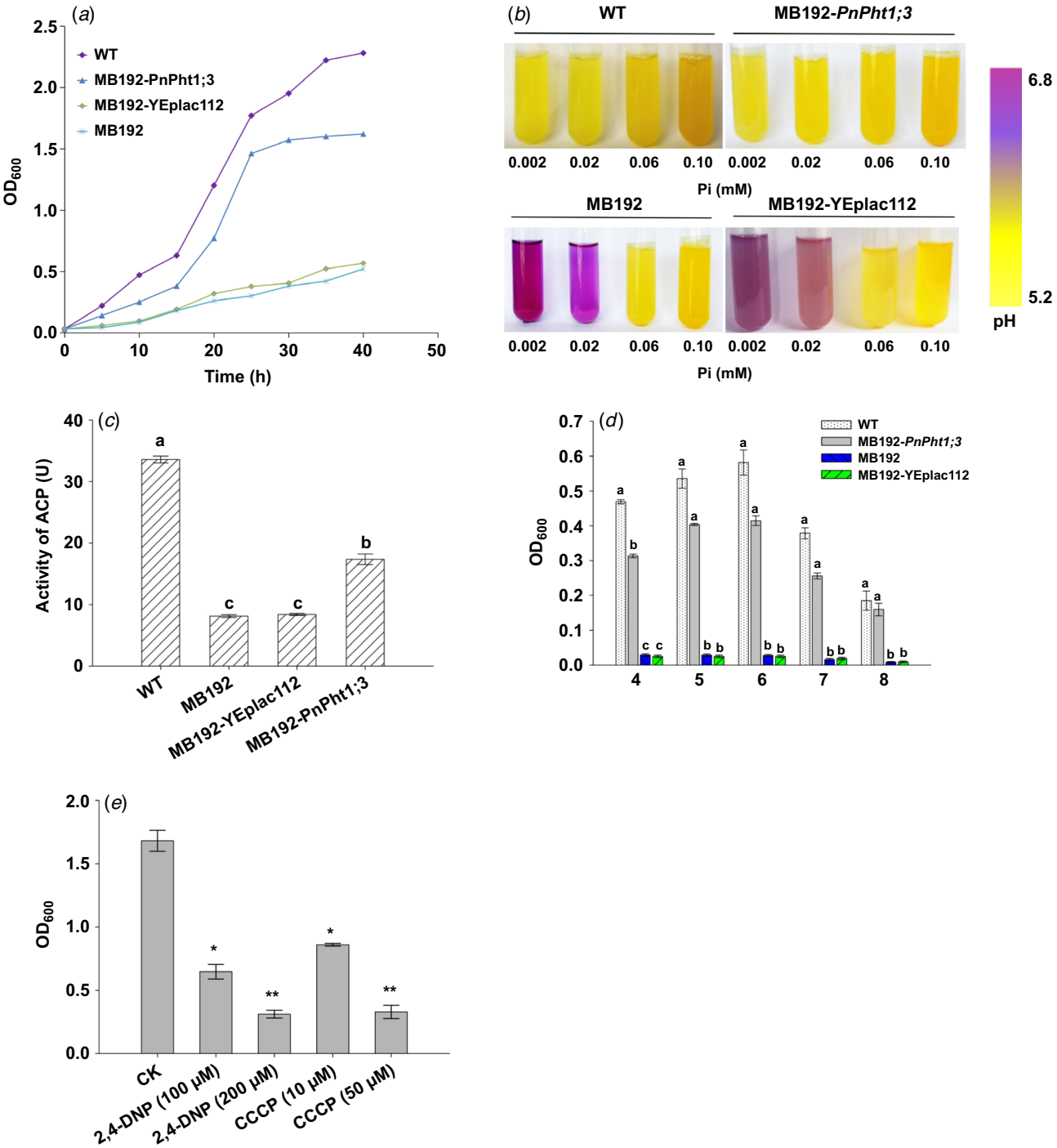

Fig. 4. Complementation assays of MB192-*PnPht1;3*. (*a*) Growth curves of WT, MB192, MB192-YEplac112 and MB192-*PnPht1;3* cultured for 40 h in the presence of low Pi (20 μM). (*b*) Medium colour changed with pH under different Pi concentrations. (*c*) ACP activity of of WT, MB192, MB192-YEplac112 and MB192-*PnPht1;3* in the presence of low Pi (20 μM) with an initial pH of 6. Different lowercase letters represent the difference of ACP activity among cells, $P \leq 0.05$. (*d*) The effect of different medium pH on the growth of WT, MB192, MB192-YEplac112 and MB192-*PnPht1;3* supplemented with 100 μM Pi. Different lowercase letters represent the difference of OD_{600} under the same pH among cells, $P \leq 0.05$. (*e*) The growth of MB192-*PnPht1;3* was suppressed by protonophores, carbonyl cyanide *m*-chlorophenylhydrazone (CCCP) and 2,4-dinitrophenol (2,4-DNP). $^{**}P \leq 0.01$; $^{*}P \leq 0.05$. Error bars indicate mean values ± s.d. ($n = 4$).

concentrations (Fig. 4e). These results confirmed that Pi transporter PnPht1;3 is a putative high-affinity $H^+/H_2PO_4^-$ symporter that mediates Pi uptake through a proton gradient generated on the membrane.

In addition, the growth rate coefficients of MB192-*PnPht1;3* and MB192-YEplac112 were calculated via exponential regression, which was based on the logarithmic phase, as shown in Fig. 5a, b. A number of independently obtained growth rate coefficients ($n = 4$) for each transporter are shown in Fig. 5c. These results showed that under low-Pi conditions (20 μM), the growth rate coefficient of MB192-*PnPht1;3* was significantly higher than that of MB192-YEplac112, suggesting Pi transporter PnPht1;3 performed optimally in complementing the yeast Pi-transport defect.

Arsenic tolerance and accumulation of yeast cells expressing *PnPht1;3*

As a common carrier, Pi transporters play important roles in the acquisition of Pi and AsV. Competitive inhibition revealed that high-concentration Pi could suppress AsV acquisition. As shown in Fig. 6, the growth curves of MB192-*PnPht1;3* and MB192-YEplac112 seemed similar in 50 μM Pi medium without AsV. Correspondingly, the growth rate coefficients of MB192-*PnPht1;3* and MB192-YEplac112 under 50 μM Pi were higher than the values determined under low-Pi (25 μM) described in the previous section. However, the growth of the two types of yeast cells was completed suppressed by supplementation with 80 μM AsV, of which the growth rate coefficients sharply decreased, e.g. 0.1588/0.0916 for MB192-*PnPht1;3* and 0.1156/0.0562 for MB192-YEplac112 (Fig. 6a, b). In contrast, the growth curve of MB192-YEplac112 was gentler than that of MB192-*PnPht1;3* under AsV stress. The As tolerance of MB192-*PnPht1;3* was assessed by calculating the percentage of growth under As exposure relative to growth in the absence of As. The results revealed that MB192-*PnPht1;3* had slightly stronger As tolerance than MB192-YEplac112. However, there was a non-significant difference between the two transgenic lines (Fig. 6c).

Under 80 μM AsV stress, the entire OD_{600} of yeast cells, including WT, MB192, MB192-*PnPht1;3* and MB192-YEplac112, increased with increasing Pi concentrations

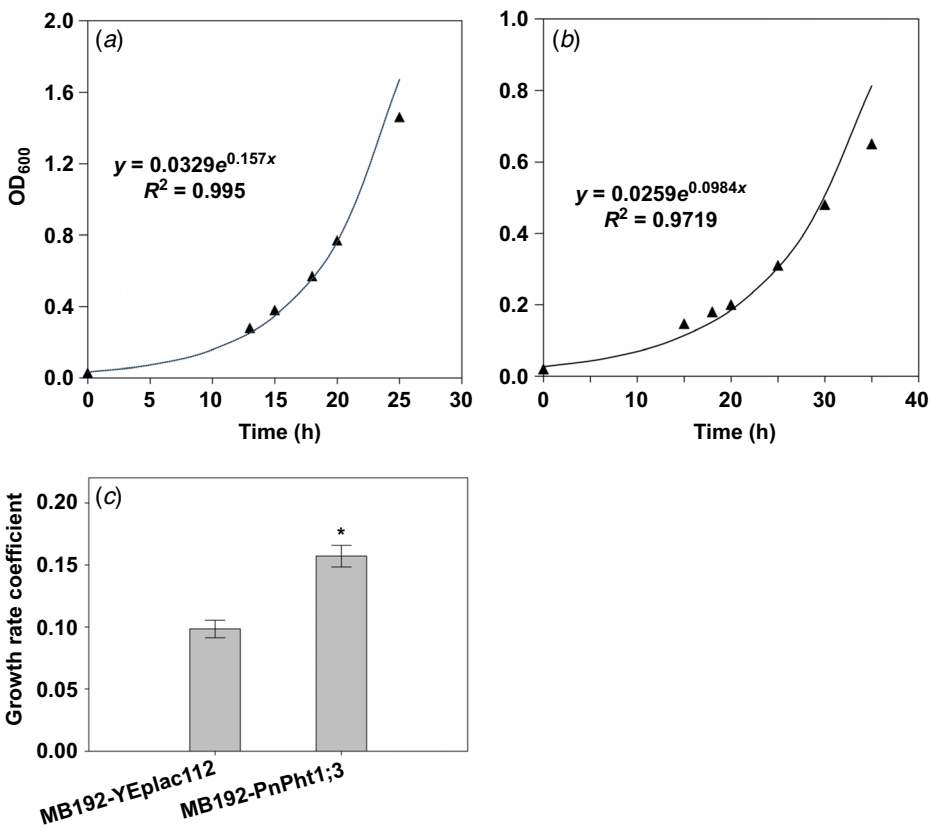

Fig. 5. Growth rate of MB192-*PnPht1;3* under a low-concentration Pi (20 μM). OD_{600} of logarithmic growth phase were used to generate exponential trend lines ($y(t) = a \times e^{kt}$), where k is the growth rate coefficient. (*a*) Growth rate of MB192-*PnPht1;3*. (*b*) Growth rate of MB192-YEplac112. (*c*) Growth rate coefficient. * represents a difference of growth rate coefficient between MB192-*PnPht1;3* and MB192-YEplac112 at $P \leq 0.05$. Error bars indicate mean values ± s.d. ($n = 4$).

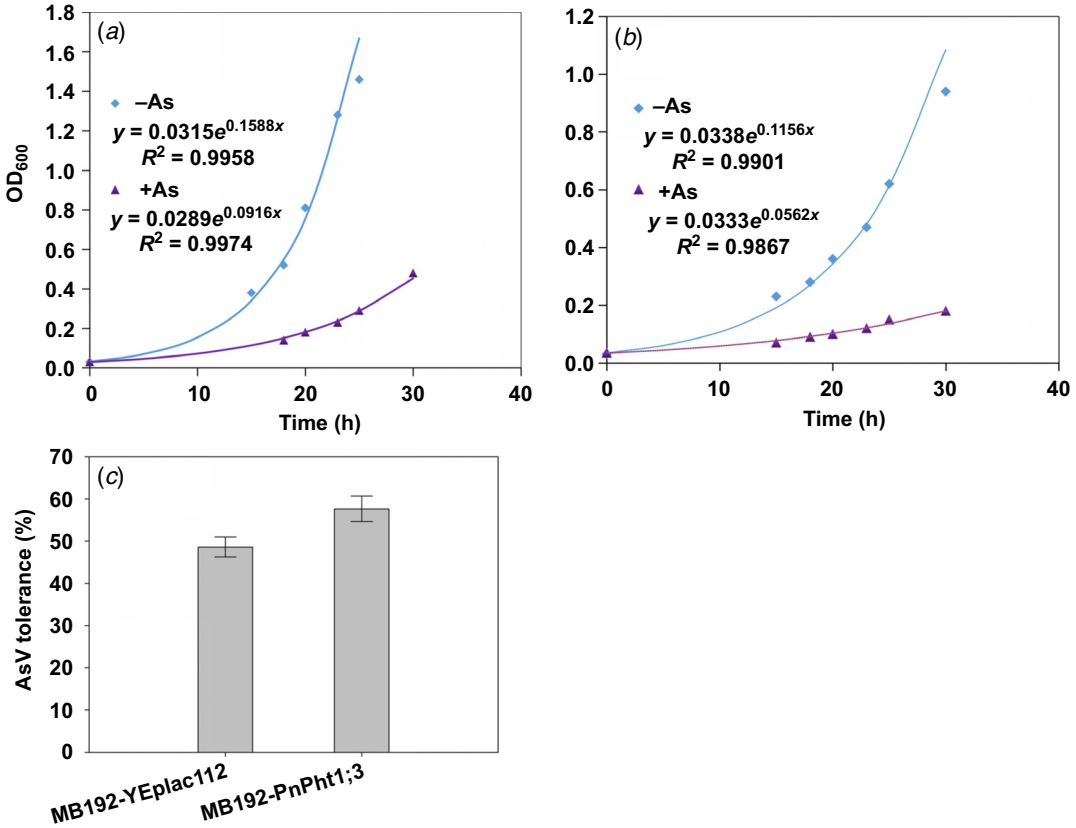

Fig. 6. Growth rates and As tolerance of MB192-*PnPht1;3* supplemented with 50 μM Pi and non-(−As) or 80 μM AsV. OD_{600} of logarithmic growth phase were used to generate exponential trend lines ($y(t) = a \times e^{kt}$), where k is the growth rate coefficient. (*a*) Growth rates of MB192-*PnPht1;3* supplement with (+As) or without (−As) 80 μM AsV. (*b*) Growth rates of MB192-YEplac112 supplement with (+As) or without (−As) 80 μM AsV. (*c*) As tolerance (%) indicates the proportional growth rate of MB192-*PnPht1;3* and MB192-YEplac112 in the presence of AsV compared with control growth. A non-significant difference of As tolerance was shown between MB192-*PnPht1;3* and MB192-YEplac112, $P > 0.05$. Values are the mean ± s.d. ($n = 4$).

from 20 to 100 μM, particularly in WT and MB192-*PnPht1;3* with a significant difference, suggesting that a high level of Pi can alleviate As stress (Fig. 7*a*). In addition, the OD_{600} of WT and MB192-*PnPht1;3* was higher than that of MB192-YEplac112 and mutant strain MB192 under the same Pi concentration (20 or 100 μM), but a non-significant difference existed between WT and MB192-*PnPht1;3*. This phenomenon demonstrates that Pi addition improved the probability that Pi transporters assimilated Pi under the competition of AsV (Cao *et al.* 2020). Another finding needs to be noted that PnPht1;3 preferred to combine Pi rather than AsV under a high concentration of Pi. These discoveries were reinforced by the result of As accumulation in yeast cells, of which the As contents of WT and MB192-*PnPht1;3* significantly decreased by the addition of high-concentration Pi, while the As accumulation of MB192-YEplac112 and mutant strain MB192 changed very little (Fig. 7*b*). Under 20 μM of Pi and 80 μM AsV stress, MB192-*PnPht1;3* had the second highest As concentration in cells and presented a significant difference from each of the four other yeast lines. When the Pi concentration reached 100 μM, the As content of MB192-*PnPht1;3* sharply decreased to a value near the level of MB192-YEplac112 and mutant strain MB192 with a non-significant difference. Taken together, although overexpression of *PnPht1;3* improved the survival of the mutant strain under Pi deficiency or AsV exposure, it could not completely complement the defect in the uptake of Pi and AsV, similar to WT. Generally, transporter PnPht1;3 has a stronger capacity for improving Pi and AsV acquisition in complementary mutants. In addition, a high Pi concentration played a positive role in alleviating AsV stress.

Discussion

P. notoginseng is a valued traditional Chinese medicinal herb. The rhizome is the main medicinal part, in which saponins are the primary bioactive components with clear

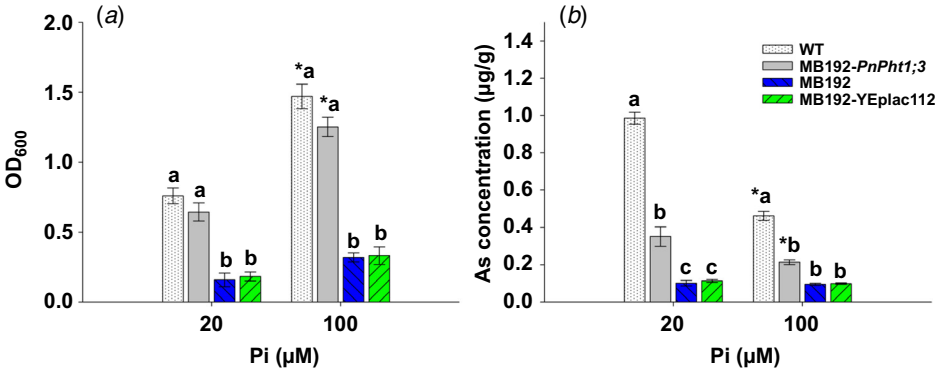

Fig. 7. Growth (*a*) and As-accumulated concentration (*b*) of WT, MB192, MB192-YEplac112, and MB192-*PnPht1;3* supplemented with low (20 μM)- or high (100 μM)-concentration Pi under the stress of 80 μM AsV. Different lowercase letters represent the difference of yeast cells under the same Pi concentration; * represents the difference of the same cell between 20 and 100 μM Pi at $P \leq 0.05$. Error bars indicate mean values ± s.d. ($n = 4$).

pharmacological effects (Feng *et al.* 2018; Zhang *et al.* 2019; Wei *et al.* 2020). Unfortunately, evidence has indicated that As contamination commonly exists in notoginseng radix – up to 56% in 31 samples (Liu *et al.* 2014*a*). Arsenic accumulation in *P. notoginseng* was mainly caused by high As concentration background of the soil. As a result, almost half of the cultivated fields experienced a crisis of excessive As in the Wenshan Prefecture, of which 21 sample plots were analysed in total (Yan *et al.* 2012). Thus, the crisis of As contamination gradually entered people's view. Consistent with reports that increasing phosphorus absorption would greatly inhibit As acquisition (Luan *et al.* 2018), our previous study found that the total As content in the notoginseng radix gradually increased with elevated AsV concentration in the soil but significantly decreased by supplementation with high-concentration Pi (Cao *et al.* 2020). These findings suggested a similar electrochemical characteristic of phosphate and AsV, whose absorption and transport were closely associated with Pi transporters (Tang *et al.* 2018). Nevertheless, the role of *P. notoginseng* Pi transporters in the uptake of Pi and As remains unclear.

Herein, the *P. notoginseng* gene *PnPht1;3* was cloned and characterised based on a transcript of *P. notoginseng* fibrous roots under the stress of Pi deficiency and AsV exposure. According to the phylogenetic tree analysis, transporter PnPht1;3 belongs to subfamily Pht1 (Fig. 1), which plays important roles in the acquisition, transport and remobilisation of Pi in plants; e.g. transporters AtPht1, AtPht2, AtPht3 and AtPht4 are mainly involved in the uptake of Pi from soil to roots in *Arabidopsis thaliana* L. (Lapis-Gaza *et al.* 2014). The responsiveness effect of plant Pht1 genes to AsV varies with regard to the specific Pht1 gene and tissue type, as well as the concentration and duration of AsV exposure (Catarecha *et al.* 2007; Puckett *et al.* 2012; LeBlanc *et al.* 2013; Muehe *et al.* 2014). Many studies have shown that Pht1 could significantly respond to the induction of Pi deficiency or As exposure, e.g. downregulation of *PvPht1;1* in *P. vittata* under As exposure, and upregulation of *PvPht1;3* in *P. vittata* under Pi deficiency or As exposure (Ditusa *et al.* 2016). Our qPCR results showed that the relative expression level of *PnPht1;3* significantly responded to both Pi deficiency and As exposure, particularly in the interaction of the two factors. The relative expression level of *PnPht1;3* sharply increased under the interaction of low Pi and As exposure, but the stress response was weakened by supplying high Pi (Fig. 3). These results indicated that PnPht1;3 preferred to combine Pi iron rather than AsV. However, the roles of *PnPht1;3* in Pi uptake and AsV accumulation remains unclear.

Hence, the characteristics of *PnPht1;3* were revealed via complementation assays in *S. cerevisiae* MB192, which was defective in the high-affinity Pi transporter. Transporter PnPht1;3 played the role of PHO84 in the uptake of Pi in MB192-*PnPht1;3* cells, which supports its growth under low Pi concentrations (2 and 20 μM Pi) (Fig. 4). Moreover, the results of pH-dependent ACP activity assays and proton pump inhibition experiments showed that PnPht1;3 was an H^+-dependent Pi transporter (Fig. 4). Correspondingly, transformant MB192-*PnPht1;3* was significantly inhibited by supplementation with CCCP or 2,4-DNP. In accordance with our results, *Catharanthus roseus* (L.) G. Don decreased cytoplasmic pH and increased pH in the extracellular medium (Sakano *et al.* 1992; Srivastava *et al.* 2018), as well as the acidification of cytoplasmic pH in the root hairs of *Limmobium stoloniferum* (G.F. Mey) Griseb. during Pi uptake, and ACP activity was improved (Sakano *et al.* 1992; Srivastava *et al.* 2018). Combined with the predicted subcellular localisation of the cytomembrane, the operation method of *PnPht1;3* could be explained by transporter PnPht1;3, as an energised transport system, via H^+/Pi co-transport to overcome the negative membrane potential entering plant cells. However, the process of $H^+/H_2PO_4^-$

symporting in the membrane has not been uncovered and is likely related to the mechanism of proton and glycerol-3-phosphate symporting in *Escherichia coli* (Abramson *et al.* 2003; Huang *et al.* 2003; Zhang *et al.* 2014).

The adaptation and tolerance of plants to As was initially uncovered at the levels of physiological and molecular mechanisms. AsV is usually reduced to AsIII in the cells of plants and further forms less toxic inorganic AsIII via methylation; e.g. dimethylarsenate (DMAsV) and trimethykarsenic oxide (TMAs) (Zhu *et al.* 2017; Alam *et al.* 2019; Roy *et al.* 2020). Arsenic only AsIII can bind to PCs and activate phytochelatin synthase, the reduction of AsV to AsIII is the first step in the detoxification of As, and As(V) reductase (AR) and its activity are therefore critical for As tolerance in plants (Li *et al.* 2016). Plant physiology changes against As stress, of which the activities of antioxidases; e.g. superoxide dismutase (SOD), catalase (CAT) and glutathione peroxidase (GPX) were improved, as well as enzymes involved in the ascorbate-glutathione (Asc-Glu) cycle and glyoxalase cycle, while the contents of antioxidants, such as proline and anthocyanin were also increased (Ahmad *et al.* 2020; Li *et al.* 2021). Many metabolic processes in plants, including availability of essential nutrients, photosynthesis, carbohydrate metabolism, lipid metabolism, protein metabolism and sulfur metabolism closely participate in As detoxification (Zhang *et al.* 2021). In addition, increasing evidence has shown that the expression levels of genes relating to transporters or phytochelate proteins are significantly upregulated; e.g. *OsLsi2*, *OsLsi1* and *OsABCC1* in rice (Abedi and Mojiri 2020; Pan *et al.* 2020). Notably, supplementation with some exogenous materies; e.g. sodium nitroprusside, melationin and Pi, would be an effective strategy for alleviating As toxicity (Ahmad *et al.* 2020; Li *et al.* 2021). Evidence has shown that high concentrations of external Pi competitively decrease the uptake and accumulation of As in plant, that could decrease membrane damage by lowering the activity of CAT, APX and lipid peroxidation (Gunes *et al.* 2009; Li *et al.* 2016). This explanation was confirmed by our previous study, in which high-concentration Pi lowered the oxidase activity of *P. notoginseng*, promoted the growth and improved the content of notoginsenoside, thereby decreasing the damage caused by AsV (Cao *et al.* 2020). Therefore, Pi application may be an important strategy for As detoxification or phytoremediation in plants and phytoplankton (Kertulis *et al.* 2005; Ye *et al.* 2011; Yan *et al.* 2012; Shaibur *et al.* 2013).

Despite the dependence on species and genotype, it could be concluded that arsenic tolerance in higher plants hinges on decreased As accumulation by suppression of the high-affinity Pi/As (V) uptake system in roots and decreased As transport to shoots (Meharg and MacNair 1992; Pigna *et al.* 2009), which is a common mechanism employed by arsenic-resistant plants (Ditusa *et al.* 2016). Thus, it is also a reasonable explanation for *PnPht1;3* that transformants of MB192-*PnPht1;3* decreased As accumulation in cells by suppression of the *PnPht1;3* uptake system under high-concentration Pi (100 μM) (Figs 6 and 7). These reports suggest that plant high-affinity Pi transporters had comparable specificities for AsV uptake and play an important role in the AsV accumulation. For example, pht1;1-3 of *A. thaliana* showed a slow rate of AsV uptake that ultimately enabled the mutant to accumulate more As under appropriate Pi levels (Anawar *et al.* 2018), while AtPht1;5 or AtPht1;7 in *A. thaliana* preferred Pi over AsV (Ditusa *et al.* 2016). Taken together, PnPht1;3 responded to the stress of Pi deficiency and As exposure and was involved in the uptake of Pi and AsV. High-concentrations of Pi could also decrease the stress of AsV.

Conclusions

PnPht1;3 cloned from the roots of *P. notoginseng* encodes a putative high-affinity Pi/H+ symport transporter protein that enhances the uptake of Pi and AsV, which may be responsible for As accumulation. The role of the Pi transporter PnPht1;3 in the acquisition of Pi and As was revealed by a series of experiments. The qPCR results showed that the relative expression level of *PnPht1;3* was significantly upregulated under Pi deficiency and AsV exposure. Heterologous expression in *S. cerevisiae* MB192 revealed that the expression of *PnPht1;3* performed optimally in complementing the yeast Pi-transport defect. In addition, As accumulation in the yeast cells could be suppressed by supplementation with Pi. Taken together, we confirmed that *PnPht1;3* encoded a functional plasma membrane-localised transporter protein that mediated putative high-affinity Pi/H^+ symport activity and enhanced the uptake of Pi and AsV, which was likely responsible for the As accumulation of *P. notoginseng*. Our results provide insight into the acquisition mechanism of As in *P. notoginseng* and strategies for reducing As accumulation in taproots for enhanced pharmacal security.

References

Abedi T, Mojiri A (2020) Arsenic uptake and accumulation mechanisms in rice species. *Plants* **9**, 129. doi:10.3390/plants9020129

Abramson J, Smirnova I, Kasho V, Verner G, Kaback HR, Iwata S (2003) Structure and mechanism of the lactose permease of *Escherichia coli*. *Science* **301**, 610–615. doi:10.1126/science.1088196

Ahmad P, Alam P, Balawi TH, Altalayan FH, Ahanger MA, Ashraf M (2020) Sodium nitroprusside (SNP) improves tolerance to arsenic (As) toxicity in *Vicia faba* through the modifications of biochemical attributes, antioxidants, ascorbate-glutathione cycle and glyoxalase cycle. *Chemosphere* **244**, 125480. doi:10.1016/j.chemosphere.2019.125480

Alam MZ, Hoque MA, Ahammed GJ, McGee R, Carpenter-Boggs L (2019) Arsenic accumulation in lentil (*Lens culinaris*) genotypes and risk associated with the consumption of grains. *Scientific Reports* **9**, 9431. doi:10.1038/s41598-019-54736-4

Anawar HM, Rengel Z, Damon P, Tibbett M (2018) Arsenic–phosphorus interactions in the soil–plant–microbe system: dynamics of uptake, suppression and toxicity to plants. *Environmental Pollution* **233**, 1003–1012. doi:10.1016/j.envpol.2017.09.098

Bun-Ya M, Nishimura M, Harashima S, Oshima Y (1991) The *PHO84* gene of *Saccharomyces cerevisiae* encodes an inorganic phosphate transporter. *Molecular and Cellular Biology* **11**, 3229–3238. doi:10.1128/mcb.11.6.3229

Cao X, Ma LQ, Shiralipour A (2003) Effects of compost and phosphate amendments on arsenic mobility in soils and arsenic uptake by the hyperaccumulator, *Pteris vittata* L. *Environmental Pollution* **126**, 157–167. doi:10.1016/s0269-7491(03)00208-2

Cao GH, Li ZD, Wang XF, Zhang X, Zhao RH, Gu W, Chen D, Yu J, He S (2020) Phosphate transporters, PnPht1;1 and PnPht1;2 from *Panax notoginseng* enhance phosphate and arsenate acquisition. *BMC Plant Biology* **20**, 124. doi:10.1186/s12870-020-2316-7

Catarecha P, Segura MD, Franco-Zorrilla JM, García-Ponce B, Lanza M, Solano R, Paz-Ares J, Leyva A (2007) A mutant of the *Arabidopsis* phosphate transporter Pht1;1 displays enhanced arsenic accumulation. *The Plant Cell* **19**, 1123–1133. doi:10.1105/tpc.106.041871

Costaglioli P, Meilhoc E, Masson JM (1994) High-efficiency electrotransformation of the yeast *Schwanniomyces occidentalis*. *Current Genetics* **27**, 26–30. doi:10.1007/BF00326575

DiTusa SF, Fontenot EB, Wallace RW, Silvers MA, Steele TN, Elnagar AH, Dearman KM, Smith AP (2016) A member of the phosphate transporter 1 (Pht1) family from the arsenic-hyperaccumulating fern *Pteris vittata* is a high-affinity arsenate transporter. *New Phytologist* **209**, 762–772. doi:10.1111/nph.13472

Doki S, Kato HE, Solcan N, Iwaki M, Koyama M, Hattori M, Iwase N, Tsukazaki T, Sugita Y, Kandori H, Newstead S, Ishitani R, Nureki O (2013) Structural basis for dynamic mechanism of proton-coupled symport by the peptide transporter POT. *Proceedings of the National Academy of Sciences of the United States of America* **110**, 11343–11348. doi:10.1073/pnas.1301079110

Feng GQ, Liu YZ, Zhang WB, Wu ZC (2005) Research on polluted channel of arsenic in the *Panax notoginseng*. *Journal of Materials Science – Materials in Medicine* **28**, 645–647. [In Chinese]. https://kns.cnki.net/kcms/detail/detail.aspx?FileName=ZYCA200508001&DbName=CJFQ2005.

Feng S, Cheng H, Xu Z, Yuan M, Huang Y, Liao J, Yang R, Zhou L, Ding C (2018) *Panax notoginseng* polysaccharide increases stress resistance and extends lifespan in *Caenorhabditis elegans*. *Journal of Functional Foods* **45**, 15–23. doi:10.1016/j.jff.2018.03.034

Gravot A, Lieutaud A, Verret F, Auroy P, Vavasseur A, Richaud P (2004) AtHMA3, a plant P_{1B}-ATPase, functions as a Cd/Pb transporter in yeast. *FEBS Letters* **561**, 22–28. doi:10.1016/S0014-5793(04)00072-9

Gunes A, Pilbeam DJ, Inal A (2009) Effect of arsenic–phosphorus interaction on arsenic-induced oxidative stress in chickpea plants. *Plant and Soil* **314**, 211–220. doi:10.1007/s11104-008-9719-9

Huang Y, Lemieux MJ, Song J, Auer M, Wang D-N (2003) Structure and mechanism of the glycerol-3-phosphate transporter from *Escherichia coli*. *Science* **301**, 616–620. doi:10.1126/science.1087619

Huang Z, An Z, Chen T, Lei M, Xiao X, Liao X (2007) Arsenic uptake and transport of *Pteris vittata* L. as influenced by phosphate and inorganic arsenic species under sand culture. *Journal of Environmental Sciences* **19**, 714–718. doi:10.1016/s1001-0742(07)60119-3

Jedynak L, Kowalska J, Kossykowska M, Golimowski J (2010) Studies on the uptake of different arsenic forms and the influence of sample pretreatment on arsenic speciation in White mustard (*Sinapis alba*). *Microchemical Journal* **94**, 125–129. doi:10.1016/j.microc.2009.10.001

Jia H, Ren H, Gu M, Zhao J, Sun S, Zhang X, Chen J, Wu P, Xu G (2011) The phosphate transporter gene *OsPht1;8* is involved in phosphate homeostasis in rice. *Plant Physiology* **156**, 1164–1175. doi:10.1104/pp.111.175240

Karandashov V, Bucher M (2005) Symbiotic phosphate transport in arbuscular mycorrhizas. *Trends in Plant Science* **10**, 22–29. doi:10.1016/j.tplants.2004.12.003

Kertulis GM, Ma LQ, MacDonald GE, Chen R, Winefordner JD, Cai Y (2005) Arsenic speciation and transport in *Pteris vittata* L. and the effects on phosphorus in the xylem sap. *Environmental and Experimental Botany* **54**, 239–247. doi:10.1016/j.envexpbot.2004.09.001

Kim J-H (2018) Pharmacological and medical applications of *Panax ginseng* and ginsenosides: a review for use in cardiovascular diseases. *Journal of Ginseng Research* **42**, 264–269. doi:10.1016/j.jgr.2017.10.004

Knudson JA, Meikle T, DeLuca TH (2003) Role of mycorrhizal fungi and phosphorus in the arsenic tolerance of *Basin wildrye*. *Journal of Environmental Quality* **32**, 2001–2006. doi:10.2134/jeq2003.2001

Lapis-Gaza HR, Jost R, Finnegan PM (2014) *Arabidopsis* PHOSPHATE TRANSPORTER1 genes *PHT1;8* and *PHT1;9* are involved in root-to-shoot translocation of orthophosphate. *BMC Plant Biology* **14**, 334. doi:10.1186/s12870-014-0334-z

LeBlanc MS, McKinney EC, Meagher RB, Smith AP (2013) Hijacking membrane transporters for arsenic phytoextraction. *Journal of Biotechnology* **163**, 1–9. doi:10.1016/j.jbiotec.2012.10.013

Lei M, Wan X, Huang Z, Chen T, Li X, Liu Y (2012) First evidence on different transportation modes of arsenic and phosphorus in arsenic hyperaccumulator *Pteris vittata*. *Environmental Pollution* **161**, 1–7. doi:10.1016/j.envpol.2011.09.017

Li H, McGrath SP, Zhao F (2008) Selenium uptake, translocation and speciation in wheat supplied with selenate or selenite. *New Phytologist* **178**, 92–102. doi:10.1111/j.1469-8137.2007.02343.x

Li N, Wang J, Song W-Y (2016) Arsenic uptake and translocation in plants. *Plant and Cell Physiology* **57**, 4–13. doi:10.1093/pcp/pcv143

Li X, He H, Zhang X, Yan X, Six J, Cai Z, Barthel M, Zhang J, Necpalova M, Ma Q, Li Z (2019) Distinct responses of soil fungal and bacterial nitrate immobilization to land conversion from forest to agriculture. *Soil Biology and Biochemistry* **134**, 81–89. doi:10.1016/j.soilbio.2019.03.023

Li X, Ahammed GJ, Zhang X-N, Zhang L, Yan P, Zhang L-P, Fu J-Y, Han W-Y (2021) Melatonin-mediated regulation of anthocyanin biosynthesis and antioxidant defense confer tolerance to arsenic stress in *Camellia sinensis* L. *Journal of Hazardous Materials* **403**, 123922. doi:10.1016/j.jhazmat.2020.123922

Lin L, Yu B, Liao X, Yan X, Zhang Y (2013) Contents and health risk of As and heavy metals in *Panax notoginseng* and their pharmaceutical preparations. *Asian Journal of Ecotoxicology* **8**, 244–249. [In Chinese]. https://kns.cnki.net/kcms/detail/detail.aspx?FileName=STDL201302017&DbName=CJFQ2013.

Liu F, Chang X-J, Ye Y, Xie W-B, Wu P, Lian X-M (2011) Comprehensive sequence and whole-life-cycle expression profile analysis of the phosphate transporter gene family in rice. *Molecular Plant* **4**, 1105–1122. doi:10.1093/mp/ssr058

Liu D, Xu N, Wang L, Cui X, , Guo L, Zhang Z, Wang J, Yang Y (2014*a*) Effects of different cleaning treatments on heavy metal removal of *Panax notoginseng* (Burk) F. H. Chen. *Food Additives & Contaminants: Part A* **31**, 2004–2013. doi:10.1080/19440049.2014.975750

Liu P, Chen S, Song A, Zhao S, Fang W, Guan Z, Liao Y, Jiang J, Chen F (2014*b*) A putative high affinity phosphate transporter, CmPT1, enhances tolerance to Pi deficiency of chrysanthemum. *BMC Plant Biology* **14**, 18. doi:10.1186/1471-2229-14-18

Livak KJ, Schmittgen TD (2001) Analysis of relative gene expression data using real-time quantitative PCR and the $2^{-\Delta\Delta Ct}$ (–Delta Delta C(T)) method. *Methods* **25**, 402–408. doi:10.1006/meth.2001.1262

López-Arredondo DL, Leyva-González MA, González-Morales SI, López-Bucio J, Herrera-Estrella L (2014) Phosphate nutrition: improving low-phosphate tolerance in crops. *Annual Review of Plant Biology* **65**, 95–123. doi:10.1146/annurev-arplant-050213-035949

Luan M, Liu J, Liu Y, Han X, Sun G, Lan W, Luan S (2018) Vacuolar phosphate transporter 1 (VPT1) affects arsenate tolerance by regulating phosphate homeostasis in *Arabidopsis*. *Plant and Cell Physiology* **59**, 1345–1352. doi:10.1093/pcp/pcy025

Mandal S, Upadhyay S, Wajid S, Ram M, Jain DC, Singh VP, Abdin MZ, Kapoor R (2015) Arbuscular mycorrhiza increase artemisinin accumulation in *Artemisia annua* by higher expression of key biosynthesis genes via enhanced jasmonic acid levels. *Mycorrhiza* **25**, 345–357. doi:10.1007/s00572-014-0614-3

Meharg AA, MacNair MR (1992) Suppression of the high affinity phosphate uptake system: a mechanism of As (V) resistance in *Holcus lanatus* L. *Journal of Experimental Botany* **43**, 519–524. doi:10.1093/jxb/43.4.519

Mimura T (1999) Regulation of phosphate transport and homeostasis in plant cells. *International Review of Cytology* **191**, 149–200. doi:10.1016/S0074-7696(08)60159-X

Mitsukawa N, Okumura S, Shirano Y, Sato S, Kato T, Harashima S, Shibata D (1997) Overexpression of an *Arabidopsis thaliana* high-affinity phosphate transporter gene in tobacco cultured cells enhances cell growth under phosphate-limited conditions. *Proceedings of the National Academy of Sciences of the United States of America* **94**, 7098–7102. doi:10.1073/pnas.94.13.7098

Muehe EM, Eisele JF, Daus B, Kappler A, Harter K, Chaban C (2014) Are rice (*Oryza sativa* L.) phosphate transporters regulated similarly by phosphate and arsenate? A comprehensive study. *Plant Molecular Biology* **85**, 301–316. doi:10.1007/s11103-014-0186-9

Ou X, Wang L, Guo L, Cui X, Liu D, Yang Y (2016) Soil–plant metal relations in *Panax notoginseng*: an ecosystem health risk assessment. *International Journal of Environmental Research and Public Health* **13**, 1089. doi:10.3390/ijerph13111089

Pan D, Yi J, Li F, Li X, Liu C, Wu W, Tao T (2020) Dynamics of gene expression associated with arsenic uptake and transport in rice during the whole growth period. *BMC Plant Biology* **20**, 133. doi:10.1186/s12870-020-02343-1

Panuccio MR, Logoteta B, Beone GM, Cagnin M, Cacco G (2012) Arsenic uptake and speciation and the effects of phosphate nutrition in hydroponically grown kikuyu grass (*Pennisetum clandestinum* Hochst). *Environmental Science and Pollution Research* **19**, 3046–3053. doi:10.1007/s11356-012-0820-5

Pigna M, Cozzolino V, Violante A, Meharg AA (2009) Influence of phosphate on the arsenic uptake by wheat (*Triticum durum* L.) irrigated with arsenic solutions at three different concentrations. *Water, Air, and Soil Pollution* **197**, 371–380. doi:10.1007/s11270-008-9818-5

Puckett EE, Serapiglia MJ, DeLeon AM, Long S, Minocha R, Smart LB (2012) Differential expression of genes encoding phosphate transporters contributes to arsenic tolerance and accumulation in shrub willow (*Salix* spp.). *Environmental and Experimental Botany* **75**, 248–257. doi:10.1016/j.envexpbot.2011.07.008

Qin L, Guo Y, Chen L, Liang R, Gu M, Xu G, Zhao J, Walk T, Liao H (2012*a*) Functional characterization of 14 Pht1 family genes in yeast and their expressions in response to nutrient starvation in soybean. *PLoS ONE* **7**, e47726. doi:10.1371/journal.pone.0047726

Qin L, Zhao J, Tian J, Chen L, Sun Z, Guo Y, Lu X, Gu M, Xu G, Liao H (2012*b*) The high-affinity phosphate transporter GmPT5 regulates phosphate transport to nodules and nodulation in soybean. *Plant Physiology* **159**, 1634–1643. doi:10.1104/pp.112.199786

Rausch C, Daram P, Brunner S, Jansa J, Laloi M, Leggewie G, Amrhein N, Bucher M (2001) A phosphate transporter expressed in arbuscule-containing cells in potato. *Nature* **414**, 462–465. doi:10.1038/35106601

Roy NK, Murphy A, Costa M (2020) Arsenic methyltransferase and methylation of inorganic arsenic. *Biomolecules* **10**, 1351. doi:10.3390/biom10091351

Rufyikiri G, Wannijn J, Wang L, Thiry Y (2006) Effects of phosphorus fertilization on the availability and uptake of uranium and nutrients by plants grown on soil derived from uranium mining debris. *Environmental Pollution* **141**, 420–427. doi:10.1016/j.envpol.2005.08.072

Sakano K, Yazaki Y, Mimura T (1992) Cytoplasmic acidification induced by inorganic phosphate uptake in suspension cultured *Catharanthus roseus* cells – measurement with fluorescent pH indicator and P-31 nuclear-magnetic-resonance. *Plant Physiology* **99**, 672–680. doi:10.1104/pp.99.2.672

Shaibur MR, Adjadeh TA, Kawai S (2013) Effect of phosphorus on the concentrations of arsenic, iron and some other elements in barley grown hydroponically. *Journal of Soil Science and Plant Nutrition* **13**, 79–85. doi:10.4067/S0718-95162013005000009

Shen J, Yuan L, Zhang J, Li H, Bai Z, Chen X, Zhang W, Zhang F (2011) Phosphorus dynamics: from soil to plant. *Plant Physiology* **156**, 997–1005. doi:10.1104/pp.111.175232

Shin H, Shin H-S, Dewbre GR, Harrison MJ (2004) Phosphate transport in *Arabidopsis*: Pht1;1 and Pht1;4 play a major role in phosphate acquisition from both low and high-phosphate environments. *The Plant Journal* **39**, 629–642. doi:10.1111/j.1365-313X.2004.02161.x

Srivastava S, Upadhyay MK, Srivastava AK, Abdelrahman M, Suprasanna P, Tran L-SP (2018) Cellular and subcellular phosphate transport machinery in plants. *International Journal of Molecular Sciences* **19**, e1914. doi:10.3390/ijms19071914

Sun D, Feng H, Li X, Ai H, Sun S, Chen Y, Xu G, Rathinasabapathi B, Cao Y, Ma LQ (2020) Expression of new *Pteris vittata* phosphate transporter PvPht1;4 reduces arsenic translocation from the roots to shoots in tobacco plants. *Environmental Science & Technology* **54**, 1045–1053. doi:10.1021/acs.est.9b05486

Tang X, Lim MP, McBride MB (2018) Arsenic uptake by arugula (*Eruca vesicaria* L.) cultivars as affected by phosphate availability. *Chemosphere* **195**, 559–566. doi:10.1016/j.chemosphere.2017.12.110

Wang J, Yang Y, Liao L, Xu J, Liang X, Liu W (2019) Genome-wide identification and functional characterization of the phosphate transporter gene family in *Sorghum*. *Biomolecules* **9**, 670. doi:10.3390/biom9110670

Wei G, Yang F, Wei F, Zhang L, Gao Y, Qian J, Chen Z, Jia Z, Wang Y, Su H, Dong L, Xu J, Chen S (2020) Metabolomes and transcriptomes revealed the saponin distribution in root tissues of *Panax quinquefolius* and *Panax notoginseng*. *Journal of Ginseng Research* **44**, 757–769. doi:10.1016/j.jgr.2019.05.009

Woolson EA, Axley JH, Kearney PC (1973) The chemistry and phytotoxicity of arsenic in soils: II. effects of time and phosphorus. *Soil Science Society of America Journal* **37**, 254–259. doi:10.2136/sssaj1973.03615995003700020028x

Wu Q, Ma X, Zhang K, Feng X (2015) Identification of reference genes for tissue-specific gene expression in *Panax notoginseng* using quantitative real-time PCR. *Biotechnology Letters* **37**, 197–204. doi:10.1007/s10529-014-1643-x

Wu Z, Ren H, McGrath SP, Wu P, Zhao F-J (2011) Investigating the contribution of the phosphate transport pathway to arsenic accumulation in rice. *Plant Physiology* **157**, 498–508. doi:10.1104/pp.111.178921

Xiong Y, Chen L, Man J, Hu Y, Cui X (2019) Chemical and bioactive comparison of *Panax notoginseng* root and rhizome in raw and steamed forms. *Journal of Ginseng Research* **43**, 385–393. doi:10.1016/j.jgr.2017.11.004

Xu J, Shi S, Wang L, Tang Z, Lv T, Zhu X, Ding X, Wang Y, Zhao FJ, Wu Z (2017) OsHAC4 is critical for arsenate tolerance and regulates arsenic accumulation in rice. *New Phytologist* **215**, 1090–1101. doi:10.1111/nph.14572

Yan X, Zhang M, Liao X, Tu S (2012) Influence of amendments on soil arsenic fractionation and phytoavailability by *Pteris vittata* L. *Chemosphere* **88**, 240–244. doi:10.1016/j.chemosphere.2012.03.015

Yan XL, Liao XY, Yu BB, Zhang WB (2011) Accumulation of soil arsenic by *Panax notoginseng* and its associated health risk. *Huan Jing Ke Xue* **32**, 880–885. doi:10.5846/stxb201307261958 [In Chinese]

Ye W-L, Khan MA, McGrath SP, Zhao F-J (2011) Phytoremediation of arsenic contaminated paddy soils with *Pteris vittata* markedly reduces arsenic uptake by rice. *Environmental Pollution* **159**, 3739–3743. doi:10.1016/j.envpol.2011.07.024

Zhang J, Hamza A, Xie Z, Hussain S, Brestic M, Tahir MA, Ulhassan Z, Yu M, Allakhverdiev SI, Shabala S (2021) Arsenic transport and interaction with plant metabolism: clues for improving agricultural productivity and food safety. *Environmental Pollution* **290**, 117987. doi:10.1016/j.envpol.2021.117987

Zhang L, Hu B, Li W, Che R, Deng K, Li H, Yu F, Ling H, Li Y, Chu C (2014) OsPt2, a phosphate transporter, is involved in the active uptake of selenite in rice. *New Phytologist* **201**, 1183–1191. doi:10.1111/nph.12596

Zhang Z, Chen L, Cui X, Zhang Y, Hu Y, Wang C, Xiong Y (2019) Identification of anti-inflammatory components of raw and steamed *Panax notoginseng* root by analyses of spectrum–effect relationship. *RSC Advances* **9**, 17950–17958. doi:10.1039/C9RA00906J

Zhu M, Zeng X, Jiang Y, Fan X, Chao S, Cao H, Zhang W (2017) Determination of arsenic speciation and the possible source of methylated arsenic in *Panax Notoginseng*. *Chemosphere* **168**, 1677–1683. doi:10.1016/j.chemosphere.2016.10.093

Zu Y, Li Z, Mei X, Wu J, Cheng S, Jiang Y, Li Y (2018) Transcriptome analysis of main roots of *Panax notoginseng* identifies genes involved in saponin biosynthesis under arsenic stress. *Plant Gene* **16**, 1–7. doi:10.1016/j.plgene.2018.08.001

Data availability. Data and material not provided in this publication or previously published are available on request to the corresponding author.

Conflicts of interest. The authors declare no conflicts of interest.

Declaration of funding. SH received stipends from the National Natural Science Foundation of China (81560612), the Yunnan Basic Research Projects (202001AT070109), the Yunnan Provincial Science and Technology Department-Applied Basic Research Joint Special Funds of Yunnan University of Chinese Medicine (202001AZ070001-010), and the Key Project at Central Government Level: The Ability Establishment of Sustainable Use for Valuable Chinese Medicine Resources (2060302-2101-24). GC received stipends from the Yunnan Basic Research Projects (2019FB122, 202101AT070608) and Yunnan Provincial Science and Technology Department-Applied Basic Research Joint Special Funds of Yunnan University of Chinese Medicine (202101AF070039). JY received a stipend from the Key Research and Development Projects of Yunnan Provincial Science and Technology Department (2019IB009).

Acknowledgements. This study was carried out with financial support from the National Natural Science Foundation of China and the Yunnan Provincial Science and Technology Department. The funding agencies had no role in the experimental design, data collection and analysis or preparation of the manuscript.

Author contributions. GC, DL, XW, XZ, XL, FZ and WG conducted the experiments, completed the statistical and data analysis. GC, WX, SH and JY wrote most of the manuscript. XW, JY and SH contributed to the experimental setup and wrote part of the manuscript. GC, JY and SH were involved in planning the experiments and wrote parts of the manuscript. All authors read and approved the manuscript.

Author affiliations

[A]School of Chinese Materia Medica and Yunnan Key Laboratory of Southern Medicine Utilization, Yunnan University of Chinese Medicine, Kunming, Yunnan 650500, China.

[B]Yunnan Key Laboratory for Dai and Yi Medicines, Yunnan University of Chinese Medicine, Kunming, Yunnan 650500, China.